INCORPORATION OF FOULING DEPOSIT MEASUREMENTS IN CRUDE OIL FOULING TESTING AND DATA ANALYSIS

***A. D. Smith[1], and E. Hitimana[1]**

[1] Heat Transfer Research Inc. (HTRI), 165 Research Dr., Navasota, TX 77868, USA, *aaron.smith@htri.net

ABSTRACT

A key challenge in interpreting crude oil fouling test rig fouling data is separating the measured overall heat transfer into a convective and a conductive contribution. In fouling rig tests, the change in convective resistance can be substantial relative to the fouling resistance; whereas in the field, this impact is less significant. To account for these effects, the measured thickness and roughness of the fouling deposits at the end of the test are used to back calculate a thermal conductivity of the deposit which is assumed constant over the test duration. With the assessed thermal conductivity, the heat transfer and pressure drop models can be reconciled to measurements by solving for the deposit thickness and roughness at each timestamp. Results also include the estimated deposit surface temperature, convective heat transfer coefficient, and the deposit's conductive resistance. This new information can be used to improve assessed fouling rate for model development. A description and demonstration of this technique are provided.

INTRODUCTION

The unwanted buildup of deposit on the heat exchanger surfaces leads to a reduction in thermal performance and increased pressure drop. Dealing with fouling leads to increased capital costs and operating expenses. To aid in understanding fouling, research test rigs are used to run controlled experiments to study the impact of operating conditions (e.g. flow, bulk temperature, wall temperature, pressure), surface shape/properties (geometry, coatings, tube alloy, etc.), and the fluid composition on fouling tendency. A key goal of fouling research is to develop models to predict the fouling rate from the operating conditions and fluid properties. One of the challenges for achieving this goal is to understand the behavior and properties of the fouling layer and the conditions at the deposit surface. To do this, techniques are needed to address the common assumption that the heat transfer coefficient at the deposit surface is constant.

Fouling resistance (R_f) is most commonly mathematically expressed as the difference in the overall heat transfer coefficient at a given point in time compared to that at a reference point time stamp (i.e. assumed clean condition; time zero) (Eq. 1). Typically, when doing experimental research, the reference point represents the beginning of steady state test conditions.

$$R_f = \frac{1}{U} - \frac{1}{U_{ref}} \tag{1}$$

For an electrically heated test section, the overall heat transfer resistance includes the convective resistance and the conductive deposit resistance (R_d) as shown in Eq. 2. To keep the terminology consistent with the traditional mathematical definition (Eq.1), "fouling resistance, R_f" will be maintained as the change in overall heat transfer resistance relative to the reference point. To make an unambiguous distinction between these two thermal resistances, the conductive thermal resistance of the deposit will be referred to as the "deposit resistance" with the corresponding symbol "R_d".

$$\frac{1}{U} = R_d + \frac{r_{clean}}{h \cdot r_{foul}} \tag{2}$$

Thus, assuming no fouling during startup, the overall heat transfer coefficient at the reference point is the same as the convective heat transfer coefficient. Thus, for in-tube flow, Eq. 1 may be expressed as shown in Eq. 3.

$$R_f = \left(R_d + \frac{r_{clean}}{h \cdot r_{foul}} \right) - \frac{1}{h_{ref}} \tag{3}$$

$$\Delta R_h = \frac{r_{clean}}{h \cdot r_{foul}} - \frac{1}{h_{ref}} \tag{4}$$

$$R_f = R_d + \Delta R_h \tag{5}$$

Because the convective heat transfer coefficient at the surface of the deposit (h) cannot be directly evaluated, it is generally required to assume the convective heat transfer coefficient change (ΔR_h) is negligible as fouling occurs and that the ratio of the clean to fouled radius is close to 1 such that Eq. 3 simplifies to $R_f = R_d$ [**1**]. Thus, the fouling resistance has become both defined by Eq. 1 and synonymous with the conductive resistance of the fouling layer; both *cannot* always be true. As Crittenden and

ISBN: 978-0-9984188-2-7; Published online www.heatexchanger-fouling.com

Alderman [**1**] explain, increased roughness of the deposit compared to the based metal and constriction of the flow path are two mechanisms that can cause the convective heat transfer coefficient (and overall heat transfer coefficient) to increase. In some cases, this increase is sufficient to observe negative fouling resistance trends.

The need to account for the impact of changing heat transfer coefficient effect has been acknowledged by other researchers [**1**], [**2**], [**3**], [**4**], [**5**]. There are four key motivations to account for the changing heat transfer coefficient and analyze fouling test rig data based on R_d rather than R_f:

1. Use of fouling models based on R_f can be misleading because it includes both the deposit resistance and a change in convective resistance. Use of fouling models based on R_d instead of R_f will avoid this concern.
2. In test rigs, where the fouling resistance is less than in the field, even a small change in convective resistance can lead to significant differences between R_f and R_d. For example, Smith et al. [**3**] illustrated that for a fouling resistance of 10^{-5} m^{2}K/W with a clean h of 1000 W/m^{2}K, a 1% change in convective resistance would lead to relative discrepancy between R_f and R_d of 100%. However, at fouling resistance over 10^{-3} m^{2}K/W, like observed in a preheat train exchangers, this difference is negligible.
3. Models based on R_d are more likely to better predict fouling in a context different than that of the test rig. The change in convective resistance is specific to a given test section geometry and test conditions. Thus, models based on R_d will be more independent of the rig-specific context and more likely to be generally applicable [**3**].
4. Accounting for the changing heat transfer coefficient results in estimates of deposit properties (thermal conductivity, thickness and roughness) as well as the conditions at the surface of the deposit (surface temperature, and heat transfer coefficient). These new layers of information provide a more complete picture of the deposit growth and surface conditions which aid our ability to understand and model the fouling.

The most notable approach to accounting for the changing convective heat transfer coefficient is the method proposed by Albert et al. 2011 [**2**] and has been extended by others [**6**], [**7**]. Because the deposit resistance and convective resistance are unknown, additional information is needed to estimate these unknowns. The approach of Albert et al. [**2**] was to use a relationship proposed by Nunner [**8**] that relates the relative change in the convective heat transfer coefficient to the relative change in friction factor raised to an exponent. Using the measured pressure drop, Albert et al. [**2**] computed a friction factor and then used the Nunner correlation to compute the convective heat transfer coefficient at the deposit surface which was then used to estimate the deposit resistance. The challenge with this approach is the friction factor computed from the pressure drop includes both the constrictive and roughness effects of the deposit. Thus, the relative change in the friction factor is higher than if the constrictive effect as accounted; this would then overestimate the increase in the convective heat transfer coefficient.

Similarly, some attempt to use pressure drop measurement to estimate the deposit thickness using a pressure drop model. This approach requires assumption of roughness (typically as smooth) and deposit surface temperature. Although this approach does provide a value to work with and gives an estimate of the deposit magnitude, it is not recommended for detailed experimental work.

This paper seeks to address these concerns by incorporating deposit measurements taken at the end of the test in the analysis. It is also a central goal of this paper to not just account for the change in the convective resistance but also to estimate the deposit thermal conductivity and the trend of the deposit thickness, roughness, and surface temperature at each timestamp.

FOULING TEST RIG AND PROCEDURE

HTRI has two high temperature fouling units (HTFU-1 & HTFU-2). These test rigs were developed to simulate fouling at operating conditions of the hottest portion of the crude preheat train. Each rig is equipped with a bulk tank, a bulk tank heater, pump, Coriolis flow meters, flow control valves, an air cooler, a hydraulic cylinder for pressure control, and a fire suppression system to allow a safe 24-hr operation.

HTFU-2 was used for 2 of the data sets presented in the Example Cases section and the HTFU-1 for the other. Functionally and test quality wise, the HTFUs are equivalent. Their differences relate to the number of test sections, physical layout, total volume, and subtleties in control schemes. Although these differences may impact the test, they are irrelevant to the application of the presented method. The HTFU-2 rig version from 2017-2020 is the most recent rig version of the three data sets and is presented here as a representative HTFU. shows the process diagram for the HTFU-2 with 4 test sections (A1, B1, B2, B3). Each flow path has a Coriolis flow meter. As shown in**Error! Reference source not found.**, each test section has inlet and outlet thermocouples, a differential pressure transducer (DPT), and a sleeved tube heated section where the fouling occurs. All HTFU-2 test sections use a 5/8-inch tube that is inserted into a large

ISBN: 978-0-9984188-2-7; Published online www.heatexchanger-fouling.com

cylinder of metal called a "sleeve" (**Error! Reference source not found.**).

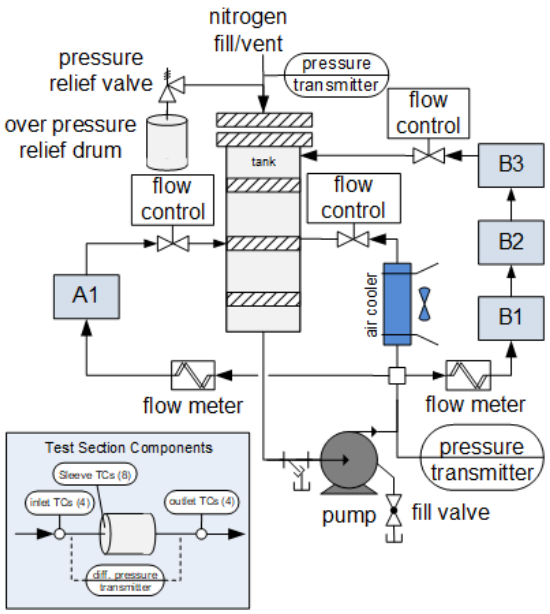

Fig. 1: HTFU-2 flow diagram

The sleeve is heated by an electrical resistance band heater. The sleeve provides more uniform heat distribution, space for thermocouples that are used to assess the inner tube wall temperature, and concentrates the heat flux. Before each test, the segment of tube between the pressure taps is replaced with a new unused tube.

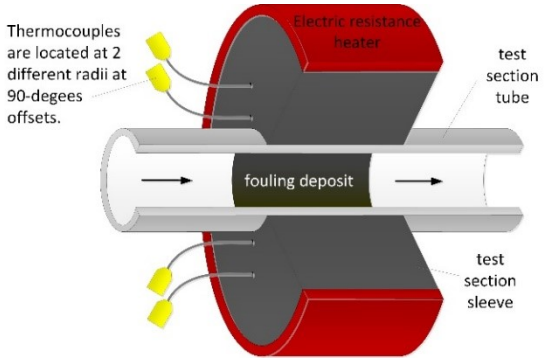

Fig. 2: Diagram of heated portion of an HTFU test section where fouling deposit is formed (drawing not to scale).

The HTFUs use an automated startup procedure to attain the pressure, flow rate, bulk temperature, and initial wall temperature set points. Once test conditions have been achieved, the mass flow rate and test section heater powers are held constant for the duration of the test. Thus, as fouling occurs the shear stress and the inside tube wall temperature will increase. Test conditions are continuously maintained without disruption until the test is ended. Typical tests have durations of 1–4 weeks. An automated shutdown procedure is used that maintains the shear stress at or below the test shear stress so as to minimize damage/erosion to the deposit. Once the rig is completely shut down, the fluid is drained and the test section tubes are removed so that the deposit may be inspected. The rig is washed with solvent and dried before each test.

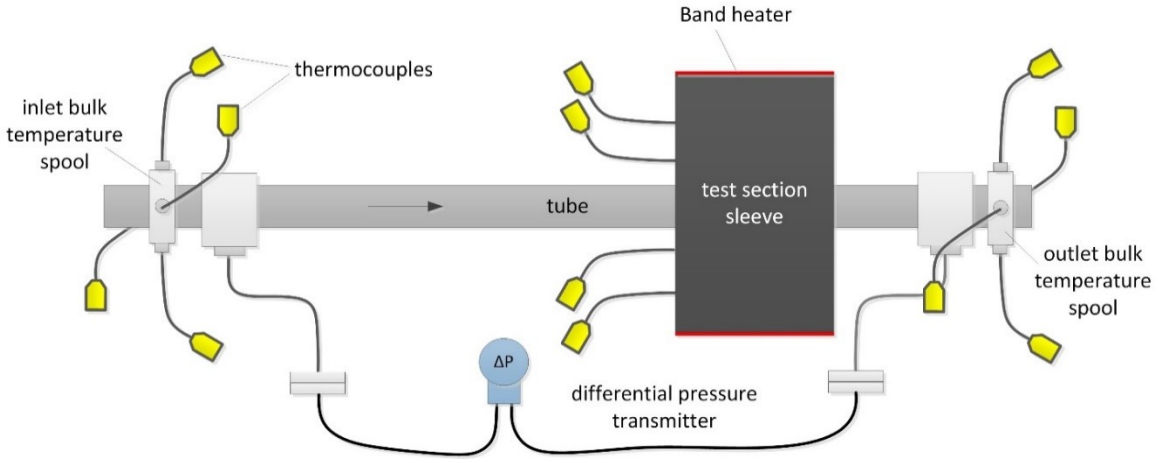

Fig. 3: Diagram of instrumentation around a single HTFU test section (drawing not to scale)

ISBN: 978-0-9984188-2-7; Published online www.heatexchanger-fouling.com

DEPOSIT THICKNESS AND ROUGHNESS MEASUREMENT

The following subsections provide an overview of the steps taken to prepare the deposit and measure its roughness and thickness.

Deposit Sample Preparation

Before the deposit thickness and roughness may be measured, the three steps are necessary to access the deposit and prepare it to be measured:

1. Cut in halves lengthwise. Fouled tubes are removed from the test rig and cut in lengthwise halves. Both tube halves are processed in the same manner described below.
2. Remove crude residue. Residual crude oil is often found at the surface of the deposit. The residual oil can adversely impact the ability of the laser to characterize the surface. To remove the residual oil, tubes are dipped into near-boiling heptane (96 – 98 °C) to decrease the viscosity of the residual crude oil on the deposit. This facilitates a free flow of the residual oil and cleaning of the surface of the deposit without dissolving the deposit
3. Scratch to expose base metal. Measuring the deposit thickness requires exposure of the bare tube metal. This is accomplished by a U-shaped scratch near the lengthwise mid-point of the deposit as shown in Fig. 4. The U-shaped scratch allows for correction of both the curvature and any tilt angle along the tube length.

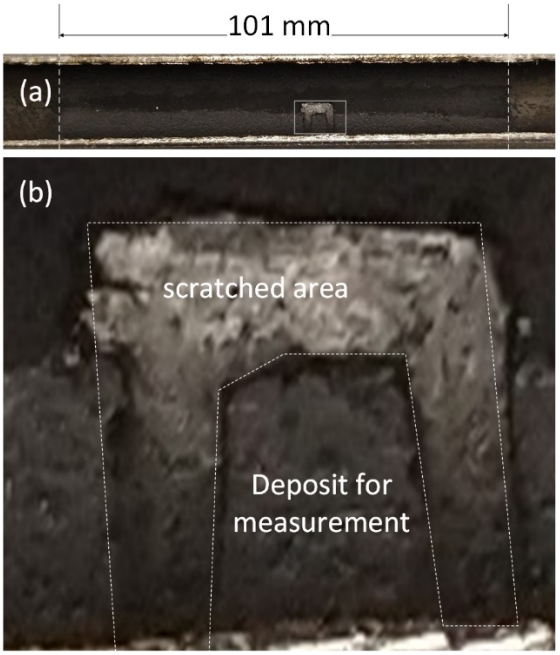

Fig. 4: Photographs of tube half with U-shaped scratch near center of the deposit. Entire deposit on tube half (a) and close up photograph of the scratched area (b).

Sample Scanning

Deposit thickness and roughness data are measured using a Keyence VK-X 110 3D laser confocal microscope equipped with a motorized stage and Nikon CF infinity-corrected 20X objective. This objective has a numerical aperture of 0.4 and a working distance of 11 mm. These optical specifications of the objective help balance between the image resolution and the total area of view. A single image is approximately 0.55 x 0.73 mm. To increase the field of view without decreasing resolution, the motorized stage is used to collect a grid of images that are then stitched together to create a single larger image. On average, the total scanned area is ~5 by ~6.5 mm which is made from 60 – 100 individual scans stitched together. Fig. 5 shows an example of the final stitched image of the deposit scan.

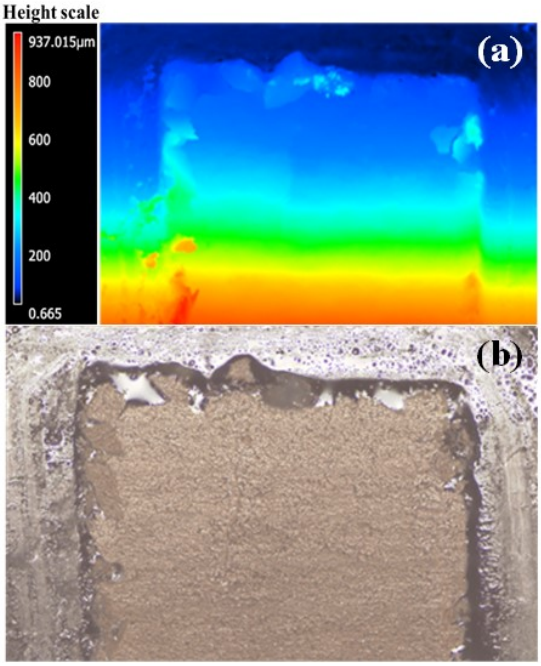

Fig. 5: Unprocessed height (a) and optical (b) images for final stitched deposit scan.

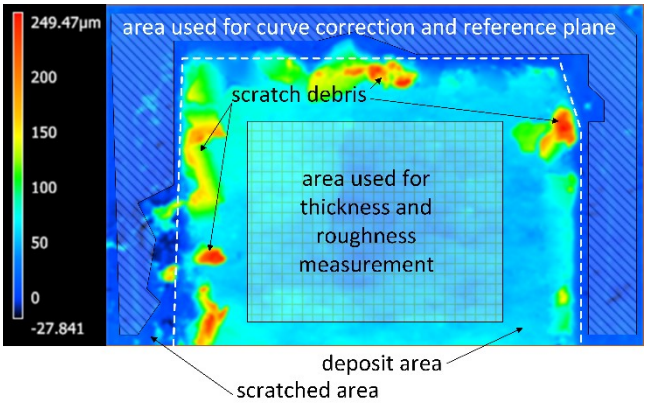

ISBN: 978-0-9984188-2-7; Published online www.heatexchanger-fouling.com

Fig. 6: A height image illustrating key areas used for processing and data analysis.

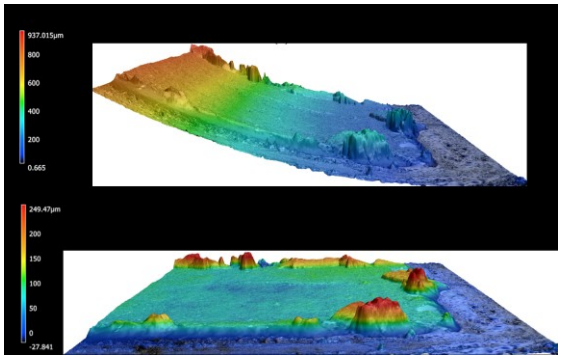

Fig. 7: 3D view of deposit scans. Before curve correction (a) and after curvature correction (b). Color bar represents the height scale.

Post processing

Prior to measuring roughness and thickness, a deposit scan must undergo a multi-step image processing so that the image is ready for analysis. Noise removal and smoothing (5x5 kernel) are done first to minimize the impact of erroneous pixels. Selection of the area used for curve correction is a manual process as care must be taken to avoid areas that do not represent the base tube metal. As shown in Fig. 6, the area for curve correction is a subset of the total scratch area as indicated by the cross-hatched area. Curve correction is then performed to transform the real surface (section of cylinder) into a flat plane (Fig. 7). The same area that is used for curve correction is also used to set the reference plane (zero elevation).

Deposit Analysis

Thickness and roughness are measured using an undisturbed area in the center of U-shaped scratch as indicated by the grid area in Fig. 6. As shown in Fig. 6, there is debris around the perimeter of the scratch area that must be avoided when selecting an evaluation area. The thickness value represents the average height difference with respect to the reference plane. The microscope software can automatically compute several different ISO roughness parameters such as arithmetic average surface roughness, S_a, used in Eq. 12 [**9**], [**10**]. The measured thickness at the length-wise center of the tube is assumed to be uniform along the length. The deposit thickness is typically greatest near the center; thus, the equivalent uniform thickness would be less which would reduce the assessed thermal conductivity.

RECONCILIATION METHOD

To determine conditions at the fouling deposit surface, there are three properties of the deposit that are needed: thickness, roughness, and thermal conductivity. Heat transfer and pressure drop models can be applied to the test section geometry which results in a system of 2 equations and 3 unknowns. An additional model or measurement is needed to enable a mathematical solution. After performing the test and measuring the deposit, the solution approach taken by HTRI is as follows:

1. Use measured end-point thickness and pressure drop and heat transfer models to solve for the deposit thermal conductivity and roughness that make the measured heat transfer and pressure drop agree with the models.
2. Assume the thermal conductivity at the end point is constant for the test duration.
3. Using the h and ΔP models, simultaneously solve for thickness and roughness that make models match measured data at all recorded timestamps.

Model details

The modelling approach used was previously outlined by Bennett and Huang [**4**]. The Churchill [**11**] friction factor was used to model the pressure drop where the roughness was that of the deposit and the hydraulic diameter was the diameter of the fouled tube (Eq. 6-9) .

$$f = f_{is}\left(\frac{\mu_w}{\mu_b}\right)^{0.14} \tag{6}$$

$$f_{is} = 2\left[\left(\frac{8}{\mathrm{Re}}\right)^{12} + \frac{1}{\left(A_1 + A_2\right)^{3/2}}\right]^{1/12} \tag{7}$$

$$A_1 = \left\{2.457\ln\left[\frac{1}{\left(\frac{7}{\mathrm{Re}}\right)^{0.9} + \frac{0.27\varepsilon_r}{D_{skin}}}\right]\right\}^{16} \tag{8}$$

$$A_2 = \left(\frac{37530}{\mathrm{Re}}\right)^{16} \tag{9}$$

Because the Gnielinski method (Eq. 10) requires uses of a smooth friction factor the Churchill friction factor was used with ε_r = 0 to compute the smooth Nusselt number. To capture the impact of roughness on heat transfer, the Norris relationship (Eq. 11) was used [**12**]. The smooth terms were computed with a roughness of zero, whereas, the fouled terms were computed using the

ISBN: 978-0-9984188-2-7; Published online www.heatexchanger-fouling.com

estimated sand-grain roughness. The flow path diameter in all equations was updated to include the thickness of the fouled layer.

$$\mathrm{Nu} = \frac{\left(\frac{f_{is}}{2}\right)\left(\mathrm{Re}-1000\right)\mathrm{Pr}_b}{1+12.7\left(\frac{f_{is}}{2}\right)^{1/2}\left(\mathrm{Pr}_b^{2/3}-1\right)}\left(\frac{\mathrm{Pr}_b}{\mathrm{Pr}_w}\right)^{0.11} \quad (10)$$

$$\left(\frac{Nu_{fouled}}{Nu_{smooth}}\right) = \left(\frac{f_{fouled}}{f_{smooth}}\right)^{0.68\mathrm{Pr}_b^{0.215}} \quad (11)$$

The Norris relationship (Eq. 11) is analogous to the Nunner relationship used by Albert et al. [**2**]; only differing by the exponent used on the friction factor ratio term. The exponent in the Norris and Nunner relationship are functions of Prandtl number; the Norris relationship results in a greater increase in heat transfer coefficient than the Nunner relationship for the same friction factor and Prandtl number. A key difference in implementation in this paper compared to Albert et al. [**2**] is that the fouled friction factor was computed according to the model with the reconciled thickness and roughness that made the model predictions match the measurements, rather than back calculating the friction factor from the measured differential pressure. Note that the calculation of the friction factor requires equivalent sand-grain roughness ($\mathcal{E}_r$) values for the smooth surface ($f_{smooth}(\mathcal{E}_r=0)$) and deposit ($f_{fouled}$). The sand-grain roughness, $\mathcal{E}_r$, is computed from measured average surface roughness parameter (S_a) using Eq. 12 [**13**]:

$$\varepsilon_r = 11.03 \cdot S_a \quad (12)$$

For an HTFU test, we presume no fouling at the reference point where, the measured overall heat transfer coefficient is the same as the convective heat transfer coefficient. Thus, unlike a double pipe test section, heat transfer models are not needed to assess the heat transfer coefficient in clean conditions. Recognizing that predicted values rarely exactly agree with measured values some compensation is required so that the reconciled answer agrees with the measurements at the reference point.

At the reference point, the ratio of the measured and predicted heat transfer coefficient and pressure drop were determined and then applied to all predicted values so that when applied at the reference point, the predictions exactly agree with the measured values as shown by Eq. 13 & 14. In this way, the solution approach places greater trust on the predicted relative change of the models to a change in thickness and roughness rather than the model's unadjusted prediction. This approach helps to compensate for inaccuracies in the model and predicted physical properties of the crude oil.

$$h_{recon.} = h_{pred}\left(\frac{h_{meas,ref}}{h_{pred,ref}}\right) \quad 13$$

$$\Delta P_{recon.} = \Delta P_{pred}\left(\frac{\Delta P_{meas,ref}}{\Delta P_{pred,ref}}\right) \quad 14$$

The heat transfer model for an HTFU consists of two resistances in series – the deposit resistance and the convective resistance as shown in Eq. 2. The deposit resistance is modelled as an annulus (Eq. 15).

$$R_d = \frac{\ln\left(\frac{r_{clean}}{r_{fouled}}\right)}{2\pi k_d L} \quad (15)$$

As shown in Eq. 16**Error! Reference source not found.**, the measured pressure drop spans over an inlet section, the heated length (sleeve), and an outlet section. The pressure drop model accounts for the unheated inlet and outlet and assumes the wall temperature in these segments is the same as the bulk temperature and that no fouling occurs. Deposit buildup is assumed to be restricted to the heated length.

$$\Delta P = \Delta P_{inlet} + \Delta P_{slv} + \Delta P_{outlet} \quad (16)$$

Limitations

Although the reconciliation method provides useful insights about the deposit's growth and surface conditions, there are limitations and considerations that should be recognized. For any test at any point during the test, the change in pressure drop and fouling resistance may increase, decrease, or remain constant compared to the reference point (9 case combinations). To understand what roughness and thickness combinations are required to achieve each of the nine scenarios, a parametric study was performed using the heat transfer and pressure drop models described above. The results are shown in Fig. 8. The mass flow rate and test section power were constant (reference point conditions). The deposit thermal conductivity was constant at the assessed value of 0.095 W/m K. The reference point operating conditions were 232 °C bulk temperature, 343°C initial wall temperature, and initial shear stress of 3.25 Pa. Thickness was varied from 0 – 100 µm and sand-grain roughness (ε_r) from 0 – 200 µm. The general trends of the pressure drop and fouling resistance isolines and shape of the illustrated regions are independent of the fluid properties and simulated operating conditions.

ISBN: 978-0-9984188-2-7; Published online www.heatexchanger-fouling.com

As indicated by the numbered comments in Fig. 8, it is observed that only six of the nine trend combinations for the change in pressure drop and fouling resistance are possible. The vast majority of the area in Fig. 8 corresponds to cases with an increasing pressure drop (Commented areas 1-3). These cases are well suited for reconciliations. Tests with no change in pressure drop and flat fouling resistance trends have no fouling (R_d = 0; Case 4 in Fig. 8). Those cases with a flat or decreasing pressure drop must have roughness that is *less* than that of the bare tube. Although this is physically possible, it is a rare occurrence. Out of 113 deposits HTRI has inspected, only 2 have had a roughness that was less than the base metal. Further, the maximum pressure drop decrease that can be obtained at zero roughness is ~5 Pa, which is practically the same as a flat pressure drop trend. For an HTFU test section, cases in which the pressure drop trend is flat or negative (|change in ΔP| < 5 Pa) the R_f and R_d will be virtually identical. This can be understood by inspection of Eq. 11; if there is no change in pressure drop, there will be no change in friction factor and, thus, no change in convective heat transfer coefficient. In these scenarios, it is reasonable to assume that R_f and R_d are equal, thickness can be computed from R_d according to Eq. 15, and roughness can be treated as constant at the value of the base material. Table I summarizes the recommended analysis approach based on the observed pressure drop and fouling resistance trend.

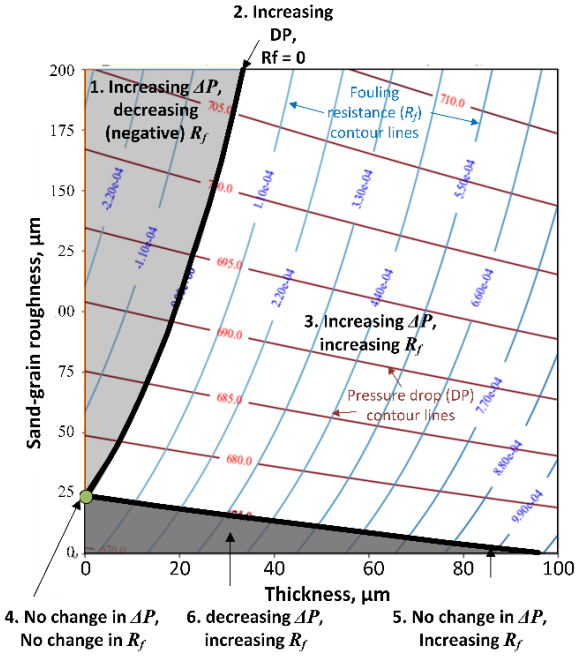

Fig. 8. Roughness and thickness parametric study with contours for pressure drop (Pa) and fouling resistance (m²K/W)

Table I: Recommended analysis for pressure drop and fouling resistance trend. The listed number corresponds to area comment indicated in Fig. 8.

	$R_f \downarrow$	$R_f = 0$	$R_f \uparrow$
ΔDP↑	reconcile, 1	reconcile, 2	reconcile, 3
ΔDP = 0	not possible	no fouling, 4	assume $R_f = R_d$, 5
ΔDP↓	not possible	not possible	assume $R_f = R_d$, 6

Because the deposit thermal conductivity is a key input to the reconciliation method, inaccuracies in the measurements used to estimate the thermal conductivity will propagate and adversely impact the overall results. In particular, thin (<10 µm; thickness on same scale as tube roughness), highly non-uniform, and/or fragile deposits can make assessment of a representative deposit thickness challenging and may lead to thermal conductivities outside a realistic range or with uncertainties greater than 100%.

The validity of assuming constant thermal conductivity remains and open question. Aging is a known phenomenon that leads to increasing thermal conductivity with time [14]. The assumption may be evaluated by conducting tests of different duration and using this method to evaluate the thermal conductivity. Compared to field heat exchangers fouling rig tests are very short, thus, significant change of deposit properties may or may not occur. Use of a thermal conductivity model would be required to account for such changes in the present method.

EXAMPLE CASES

Table II: Crude oil properties

Property	ASTM Method	Crude A	Crude B
API gravity	D287	20.0°	21.0°
Kinematic viscosity, 50 °C	D445	54.2 cSt	58.7 cSt
Heptane insoluble, wt %	D3279	7.0%	10.8%
Sulfur, wt%	D4294	2.2%	3.71%
Thermal conductivity, 260 °C	D7984	0.15	0.16
Thermal conductivity, 371 °C	D7984	0.13	0.15
Prandtl number, 260 °C	n/a	8.87	3.64

For each of the scenarios where the reconciliation method is recommended (Areas 1 – 3 in Fig. 8), an example test case is provided. Two of

ISBN: 978-0-9984188-2-7; Published online www.heatexchanger-fouling.com

these cases were with Crude A and the other with Crude B. Properties of these two crudes are shown in Table II. In all three cases, new seamless SA179 carbon steel tubes were used. The average roughness (S_a) [**10**] for these tubes is 2.15 µm. The equivalent sand-grain roughness of 23.71 µm (Eq. 12) was used as the clean tube roughness.

Case 1 – increased Δ P with positive R_f

This test was with Crude A and corresponds to Area 3 in Fig. 8. The test conditions and measured deposit properties are shown in Table III and Table IV, respectively. The measured and reconciled results for Case 1 are shown in Fig. 9., from which, it can be observed that the pressure drop and fouling resistance increase with time. The fouling resistance initially has an accelerating trend that reaches an apex. This apex is followed by a decrease over a few days after which there is steady increase for the remainder of the test duration. It is unclear if this fouling resistance trend is a result of a removal event or a rapid change in the convective resistance at the surface of the deposit. Upon inspection of the Rd, thickness (thk) and ΔRh it is observed that the decrease in the Rf is a combination of removal (decreased thickness; decreased Rd) and a decrease in convective resistance (ΔRh). This is reasonable considering that the removal of material is likely to, at least temporarily, increase roughness.

Table III: Test conditions for Case 1

Test Condition	Value
Initial wall temp. °C	372
Heater power, W	522
Bulk temperature, °C	263
Velocity, m/s	0.76
Reynolds number	8648
Initial shear stress, Pa	1.67
Initial pressure drop, Pa	605.2
Pressure drop increase at end of test, Pa	43.8
Inlet pressure, kPa (absolute)	4313

Table IV. Case 1 deposit properties

Parameter	Value
Measured thickness	64 µm
Measured avg. roughness, S_a	21.1 µm
Sand-grain roughness (Eq. 12)	233 µm
Estimated deposit thermal conductivity from end point data	0.087 W/mK

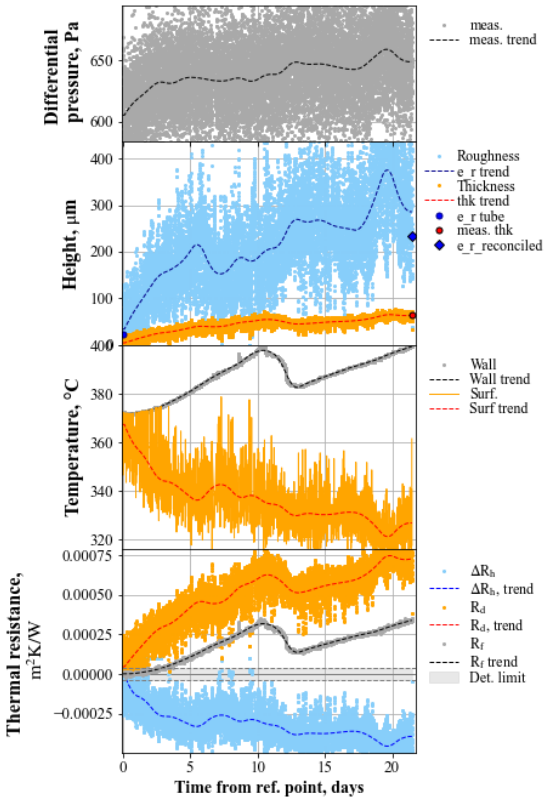

Fig. 9: measured (gray) and reconciled results (orange and blue) for Case 1

It is also observed in Fig. 9 that the surface temperature of the deposit decreases from the initial wall temperature while, at the same time, the wall temperature increases. This is contrary to the common assumption that for constant power/flux tests the surface temperature is the same as the initial wall tempertature.

The deposit resistance (R_d) trend is greater than the R_f trend and has a more asymptotic shape. The initial rate of the R_d curve is clearly higher than that of R_f. The decreasing rate (asymptotic shape) of the R_d curve is at least partially explained by the insight that the surface temperature is decreasing.

It is also notable that the reconciled sand-grain roughness ("e_r_reconciled" in Fig. 9) at the end point is 286 µm which is within ~20% of the estimated value (233 µm, Eq. 12) using the measured S_a and Eq. 12. Unlike the reconciled thickness which is forced to agree via the estimated thermal conductivity, the algorithm does not force the roughness to agree with the measurement.

Case 2 – increased Δ P with near zero R_f

This test was with Crude B and is a case corresponding to Area 2 in Fig. 8. The test conditions and measured deposit properties are shown in

Table V and **Error! Reference source not found.**, respectively.

ISBN: 978-0-9984188-2-7; Published online www.heatexchanger-fouling.com

Table V: Test conditions for Case 2

Test Condition	Value
Initial wall temp. °C	371.6
Heater power, W	452
Bulk temperature, °C	263
Velocity, m/s	0.706
Reynolds number	8351
Initial shear stress, Pa	1.78
Initial pressure drop, Pa	574.2
Pressure drop increase at end of test, Pa	14.9
Inlet pressure, kPa (absolute)	3098

Table VI. Case 2 deposit properties

Parameter	Value
Measured thickness	16.3 µm
Measured avg. roughness, S_a	7.1 µm
Sand-grain roughness (Eq.10)	78 µm
Estimated deposit thermal conductivity from end point data	0.08 W/mK

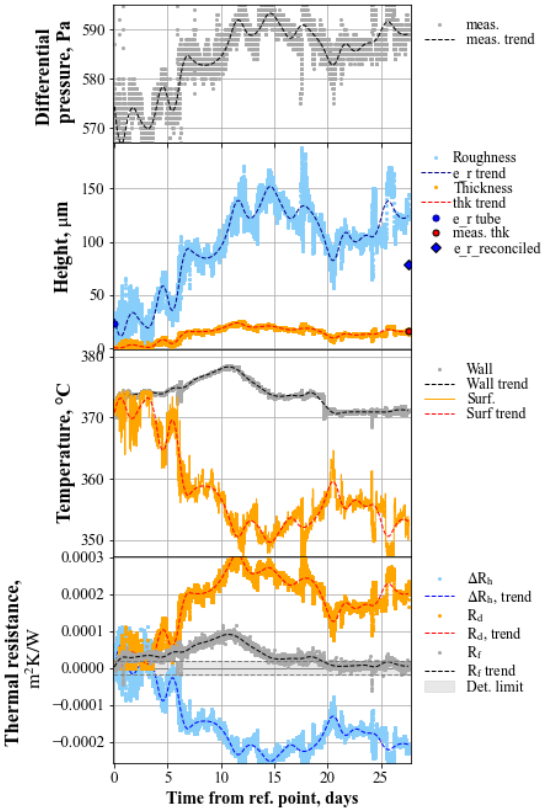

Fig. 10: measured (gray) and reconciled results (orange and blue) for Case 2

The measured and reconciled results are shown in **Error! Reference source not found.**. In this case, the R_f increases and then decreases to near zero at the end of the test. Prior to reconciliation, this would imply that the deposit had been removed. However, a thin deposit thickness of 16 µm was measured, thus, the deposit resistance cannot be zero. From reconciliation, it is observed that although some deposit was removed (decreased thickness) the deposit resistance did not go to zero but was negated by the decrease in convective resistance (ΔR_h). Like Case 1, similar comparisons of the wall temperature and surface temperature as well as the R_d and R_f are observed.

The reconciled sand-grain roughness at the end point was 124 µm. Although this is ~60% greater than the measured thickness of 78 µm it is of a similar magnitude. Trend wise, both the measured and reconciled roughness agree in that roughness increased compared to the base metal supporting the insight that convective resistance increased.

Case 3 – increased Δ P with negative R_f

This test was with Crude A and is a case corresponding to Area 1 in Fig. 8. The test conditions and deposit properties are shown in Table VII and Table VIII, respectively. Case 3 was performed before HTRI had the capability to measure the deposit thickness and roughness. For this case the deposit thermal conductivity of Case 1, which was also Crude A, was used.

Table VII: Test conditions for Case 3

Test Condition	Value
Initial wall temp. °C	318.5
Heater power, W	190
Bulk temperature, °C	271
Velocity, m/s	0.69
Reynolds number	8304
Initial shear stress, Pa	1.46
Initial pressure drop, Pa	425.2
Pressure drop increase at end of test, Pa	4.2
Inlet pressure, kPa (absolute)	1857

Table VIII. Case 3 deposit properties

Parameter	Value
Measured thickness	unavailable
Measured avg. roughness, S_a	unavailable
Sand-grain roughness (Eq. 12)	n/a

ISBN: 978-0-9984188-2-7; Published online www.heatexchanger-fouling.com

Deposit thermal conductivity from Case 1	0.09 W/mK

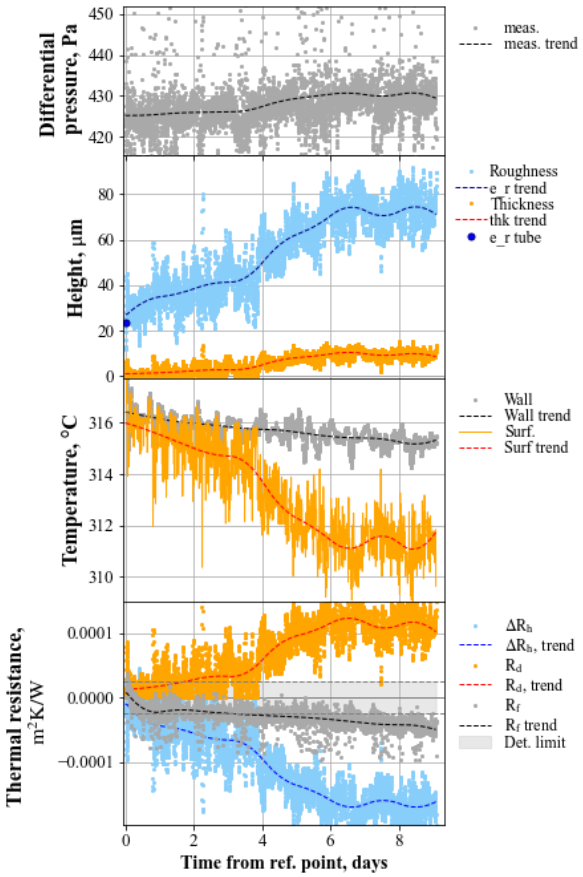

Fig. 11: measured (gray) and reconciled results (orange and blue) for Case 3

Fig. 11 shows the measured and reconciled results for Case 3. The pressure drop trend has a subtle but increasing trend (~5 Pa) and the R_f has a negative trend. Just as has been described by others [**1**] [**2**], we observe how increase roughness and constriction can increase the heat transfer coefficient (decrease ΔR_h) such that negative fouling resistances can be observed even though there is a fouling deposit layer.

General Observations from Cases 1-3

From these cases (and many other cases HTRI has studied) the following general trends are observed:

- The deposit resistance (R_d) is generally greater than the fouling resistance (R_f) because the constriction and increased roughness decrease the convective resistance. Contrary to typical research practice, R_f and R_d can only be assumed to be equal when there is no change in pressure drop over the test.
- The deposit thermal conductivity (k_d) measured values are all in the order of 0.1 W/mK, which is lower than expected and that of the oil. A common approach to estimating deposit thermal conductivity is to use R_f (not R_d) and thickness estimated from pressure drop ignoring roughness because roughness information is unavailable. By comparison, the method presented here would result in a lower k_d as R_d is greater than R_f and ignoring roughness would overstate the thickness. It should also be pointed out that there is a great deal of uncertainty with the deposit measurement due to use of a small area and assuming it represents the entire deposit; the real thickness could be significantly different. Because of the limited area measured and the fact that the scratching technique does not always expose clean tube metal; thus the deposit thickness may be larger than measured. Also, the rinsing step while necessary to remove oil could remove some deposit leading to a lower k_d. It has also been observed that many deposits have a porous structure as is evident by "bleeding" of crude oil from the deposit when scratched. Its possible that this porous structure reduces the thermal conductivity. Concerns related to deposit thickness measurement are significant enough that these concerns should be address first.
- Surprisingly, fixed power runs actually have significantly decreasing surface temperatures from the initial wall temperature.
- Roughness increases as thickness increases
- Heat transfer coefficient increases introducing a decrease in the convective resistance
- For tests run at constant power, the surface temperature of the deposit generally decreases as the fouling layer grows even though the wall temperature increases; this can partially explain the common observation of asymptotic (decreasing fouling rate) fouling trends.

Table IX shows the estimated initial fouling rates that are obtained from R_f and R_d for each case. It is clear that rate based on R_d is significantly greater than those from R_f. This will obviously impact models developed and fit to these data. As stated in the Introduction, models based on R_d are considered to be more generally applicable as the impact of changing heat transfer coefficient is very specific to test rig and geometry. By performing reconciliation these rig specific impacts are accounted.

Table IX. Comparison of the estimated initial fouling rates from R_f and R_d for each case

Case	dR_f/dt, m²K/Wd	dR_d/dt, m²K/Wd	Ratio of dR_d/dt to dR_f/dt
1	3.43E-05	1.08E-04	3.1
2	9.00E-07	2.50E-05	27.8
3	negative	2.08E-06	Negative to positive

ISBN: 978-0-9984188-2-7; Published online www.heatexchanger-fouling.com

In all three cases, there are fluctuations in the fouling resistance that may lead to speculation of causation. Application of reconciliation provides some estimate of the relative contributions of increased roughness versus removal (decreased thickness).

CONCLUSIONS

- Deposit thickness and roughness measurements provide additional data to interpret thermal and pressure drop measurements.
- Reconciliation of thermal and pressure drop models to measurements provides a method to estimate deposit properties and deposit surface conditions over the course of the test provides greater insight to understand the fouling process.
- Fouling rates assessed from R_f will be typically be underestimated compared to those made from R_d estimates.
- Based on HTRI's HTFU crude oil fouling tests, deposit roughness generally increases with deposit thickness.
- General agreement of the magnitude of the reconciled and calculated (ε_r from measured S_a; Eq. 12) sand-grain roughness suggests that Eq. 12 is a reasonable method to convert measure surface roughness parameters to sand-grain roughness.

RECOMMENDATIONS

Based on this work, the following are recommendations for future research.

- Measure the deposit thickness and roughness at the conclusion of each test.
- Increase the area of deposit inspected to reduce uncertainty of these key measurement and inputs to the reconciliation analysis.
- Investigate the spatial variations in local deposit thickness and roughness in comparison with measurement over the entire deposit area.
- Improve test section designs so that pressure drop increase is more sensitive to fouling.
- Improve, develop and confirm methods to translate measured roughness to sand-grain roughness.
- Investigate correlations to predict deposit roughness from deposit thickness, fluid properties, and/or test conditions.
- Investigate methods to predict deposit thermal conductivity.
- Investigate impact of reconciled results using alternate heat transfer and pressure drop correlations.

NOMENCLATURE

A_1	Correlation parameter, dimensionless
A_2	Correlation parameter, dimensionless
D_{skin}	Inside diameter to surface, m
f	Friction factor, dimensionless
h	Convective heat transfer coefficient at surface of the deposit, W/m^{2}K
k_d	Deposit thermal conductivity, W/m K
k_{oil}	Oil thermal conductivity, W/m K
L	Length of heated area, m
Nu	Nusselt number, dimensionless
Pr_b	Prandtl number of bulk fluid, dimensionless
Pr_w	Prandtl number of fluid at the heated surface, dimensionless
r_{clean}	Clean inside radius of tube, m
r_{foul}	Inside radius of fouling deposit, m
Re	Reynolds number, dimensionless
R_d	Fouling deposit resistance, m^{2}K/W
R_f	Fouling resistance, m^{2}K/W
S_a	Arithmetic average surface roughness, m
T	Temperature, °C
U	Overall heat transfer coefficient, W/m^{2}K

Greek Letters

μ_b	Bulk viscosity, Pa s
ε_r	Sand-grain surface roughness, m
ΔP	Pressure drop, Pa
ΔR_h	Change in convective resistance, m^{2}K/W
μ_w	Wall viscosity, Pas

Subscript

fouled	Evaluated at inside radius and roughness of the fouled surface
inlet	Inlet segment of the test section
is	Isothermal
meas.	Measured value
meas, ref	Measured value at reference point
outlet	Outlet segment of the test section
pred, ref	Predicted value at reference point
pred	Predicted value
recon.	Reconciled value
ref	Reference point
slv	Heated portion of the test section as defined by length of sleeve
smooth	Evaluated at inside radius of the clean tube with a smooth surface (zero roughness)
w	Wall

REFERENCES

ISBN: 978-0-9984188-2-7; Published online www.heatexchanger-fouling.com

1. B. Crittenden and N. J. Alderman, Mechanisms by which fouling can increase overall heat transfer, *Heat Transfer Engineering* **13**(4), 32-41 (1992).
2. F. Albert, W. Augustin, and S. Scholl, Roughness and constriction effects on heat transfer in crystallization fouling, *Chemical. Eng. Sci.* **66**, 499-509 (2011).
3. A. D. Smith, E. M. Ishiyama, J. S. Harris, and M. R. Lane, Translating crude oil fouling testing rig data to the field: A road map for future research, in *Proc. Intel. Conf Heat Exchanger Fouling and Cleaning SII*, 14-24 (2017).
4. C. A. Bennett and L. Huang, Intube fouling: effects of roughness and deposit thermal conductivity, F-19, Heat Transfer Research, Inc., Navasota, TX (2009).
5. F. Schluter, W. Augustin, and L. Scholl, Applications of experimnental data to model local fouling resistances, *Heat and Mass Transfer* **58**, 29-40 (2022).
6. B. O. Hasan, E. A. Jwair, and R. A. Craig, The effect of heat transfer enhancement on the crystallization fouling in a double pipe heat exchanger, *Experimental Thermal and Fluid Science* **86**, 272-280 (2017).
7. Y. Lv, K. Lu, and Y. Ren, Composite crystallization fouling characteristics of normal solubility salt in double-pipe heat exchanger, *International Journal of Heat and Mass Transfer* **156**, 119883 (2020).
8. W. Nunner, Warmeubergang und Druckabfall in rauen Rohen, in *VDI Forschungsheft 455*, Dusseldorf (1956).
9. L. Tonietto, L. Gonzaga Jr., M. R. Veronez, C. Kazmierczak, C. M. Arnold, and C. Andre da Costa, New method for evaluating surface roughness parameters acquired by laser, *Scientific reports* **9**(1), 1-6 (2019).
10. Keyence Corporation, Laser Scanning Microscope Reference Manual, 2018.
11. S.W Churchill, Friction-factor equation spans all fluid-flow regimes, *Chemical Engineering* **84**, 91-92 (1977).
12. R. H. Norris, Some simple-approximate heat transfer correlations for turbulent flow in ducts with rough surfaces, in *Augmentation of convective heat and mass transfer*, 16-26 (1970).
13. T. Adams and C. Grant, A Simple Algorithm to Relate Measured Surface Roughness to Equivalent Sand-grain Roughness, *International Journal of Mechanical Engineering and Mechatronics* **1**(1) (2012).
14. E. M. Ishiyama, E. Falkeman, I. Wilson, and S. J. Pugh, Quantifying Implications of Deposit Aging from Crude Refinery Preheat Train Data, *Heat Transfer Engineering*, 115-126 (2019).
15. A. P. Watkinson, Critical review of organic fluid fouling, ANL/CNSV-TN-208., Argonne National Laboratory: US Department of Energy (1988).
16. P. Singh, R. Venkatesan, H. Fogler, and N. Nagarajan, Formation and ageing of incipient thin film wax-oil gels, *AICHE Journal* **46**, 1059-1074

ISBN: 978-0-9984188-2-7; Published online www.heatexchanger-fouling.com